CSIRO PUBLISHING

Reproduction, Fertility and Development, 2019, **31**, 482–495
https://doi.org/10.1071/RD18218

Morphometric and gene expression analyses of stromal expansion during development of the bovine fetal ovary

M. D. Hartanti[A], *K. Hummitzsch*[A], *H. F. Irving-Rodgers*[A,B], *W. M. Bonner*[A], *K. J. Copping*[A], *R. A. Anderson*[C], *I. C. McMillen*[D], *V. E. A. Perry*[E] and *R. J. Rodgers*[A,F]

[A]Discipline of Obstetrics and Gynaecology, School of Medicine, Robinson Research Institute, The University of Adelaide, Adelaide, SA 5005, Australia.
[B]School of Medical Science, Griffith University, Gold Coast Campus, Qld 4222, Australia.
[C]Medical Research Council Centre for Reproductive Health, University of Edinburgh, Edinburgh, EH16 4TJ, UK.
[D]The Chancellery, University of Newcastle, Callaghan, NSW 2308, Australia.
[E]School of Veterinary and Medical Science, University of Nottingham, Sutton Bonington, LE12 5RD, UK.
[F]Corresponding author. Email: ray.rodgers@adelaide.edu.au

Abstract. During ovarian development stroma from the mesonephros penetrates and expands into the ovarian primordium and thus appears to be involved, at least physically, in the formation of ovigerous cords, follicles and surface epithelium. Cortical stromal development during gestation in bovine fetal ovaries ($n = 27$) was characterised by immunohistochemistry and by mRNA analyses. Stroma was identified by immunostaining of stromal matrix collagen type I and proliferating cells were identified by Ki67 expression. The cortical and medullar volume expanded across gestation, with the rate of cortical expansion slowing over time. During gestation, the proportion of stroma in the cortex and total volume in the cortex significantly increased ($P < 0.05$). The proliferation index and numerical density of proliferating cells in the stroma significantly decreased ($P < 0.05$), whereas the numerical density of cells in the stroma did not change ($P > 0.05$). The expression levels of 12 genes out of 18 examined, including osteoglycin (*OGN*) and lumican (*LUM*), were significantly increased later in development ($P < 0.05$) and the expression of many genes was positively correlated with other genes and with gestational age. Thus, the rate of cortical stromal expansion peaked in early gestation due to cell proliferation, whilst late in development expression of extracellular matrix genes increased.

Additional keywords: extracellular matrix, proliferation, stroma.

Received 9 June 2018, accepted 18 August 2018, published online 3 December 2018

Introduction

Connective tissue or stroma plays an important role in the formation of the ovary and during folliculogenesis as shown in mouse (Weng *et al.* 2006), cow (Wandji *et al.* 1996) and human (Heeren *et al.* 2015). Ovarian stroma contains fibroblasts and extracellular matrix. The matrix contains reticular fibres (Bandeira *et al.* 2015), fibrillar collagens (Iwahashi *et al.* 2000; Hummitzsch *et al.* 2013, 2015), decorin (Hummitzsch *et al.* 2013, 2015), fibronectin (Hummitzsch *et al.* 2013, 2015), versican (McArthur *et al.* 2000; Hummitzsch *et al.* 2013, 2015), fribillins (Prodoehl *et al.* 2009; Hatzirodos *et al.* 2011; Hummitzsch *et al.* 2013, 2015; Bastian *et al.* 2016), latent transforming growth factor β (TGFβ)-binding proteins (Prodoehl *et al.* 2009; Hatzirodos *et al.* 2011; Bastian *et al.* 2016) and hyaluronan (Kobayashi *et al.* 1999; Irving-Rodgers and Rodgers 2007). Stromal extracellular matrix components have been linked to the growth and maturation of follicles in sheep (Huet *et al.* 2001) by maintaining the shape of granulosa cells as well as their survival and proliferation *in vitro*.

The ovarian stroma is initially derived from the underlying mesonephros and infiltrates the genital ridge composed of the somatic gonadal ridge epithelial-like (GREL) cells and primordial germ cells–oogonia (Hummitzsch *et al.* 2013). When stroma first penetrates the ovaries, it is vascularised with capillaries. As it penetrates towards the surface of the ovary primordium the stroma branches and thus corrals the germ cells and somatic GREL cells into forming the ovigerous cords. This region containing the ovigerous cords and the branches of stroma becomes the cortex of the ovary, while the medullary area is substantially mesonephric stroma containing the rete

derived from mesonephric ducts. Later, commencing at the medullary–cortical interface, primordial follicles are formed and some become activated and develop further into primary and preantral follicles (Sarraj and Drummond 2012; Smith *et al.* 2014). As the stroma reaches to below the ovarian surface, it expands laterally below the surface sequestering a population of GREL cells underlain by a basal lamina at the interface (Hummitzsch *et al.* 2013); the hallmark of an epithelium. At the final stage of ovarian development, the stroma just below the surface develops into the avascular, collagen-rich tunica albuginea.

Many changes in gene expression occur during fetal ovarian development, such as expression of the pluripotency marker POU class 5 homeobox 1 (*POU5F1* or *Oct4*), deleted in azoospermia-like (*DAZL*), forkhead box L2 (*FOXL2*), as well as members of the TGF family including *TGFB1*, *2* and *3*, activins, inhibins and bone morphogenetic proteins (*BMP*s; reviewed in Sarraj and Drummond 2012). The ovarian stroma is potentially influenced by several factors, including members of the TGFβ pathway (Roy and Kole 1998; Bastian *et al.* 2016) and androgens and oestrogens (Abbott *et al.* 2006; Loverro *et al.* 2010). Abnormal development of ovarian stroma could potentially lead to an altered stromal volume in adulthood, as observed in polycystic ovary syndrome (PCOS; Hughesdon 1982; Fulghesu *et al.* 2001; Abbott *et al.* 2006; Li and Huang 2008). Despite the importance of stroma, it is probably the least studied compartment of the ovary. Using the bovine ovary, which is similar to the human ovary (Adams and Pierson 1995; Kagawa *et al.* 2009), including fetal ovarian development (Hatzirodos *et al.* 2011), stereometric and gene expression analyses were undertaken to evaluate stromal development and the expression of several genes respectively, in relation to major histological changes during the development of the ovary.

Materials and methods

Abattoir ovary collection

Bovine fetal ovarian pairs ($n = 27$) from different stages of development were collected from pregnant *Bos taurus* cows from a local abattoir (Thomas Foods International) and crown–rump length (CRL) was measured to estimate the gestational age (Russe 1983). All samples were transported to the laboratory on ice in Hank's balanced-salt solution containing Mg^{2+} and Ca^{2+} ($HBSS^{+/+}$; Sigma-Aldrich Pty Ltd, Australia). To determine the sex of fetuses with CRL <10 cm in order to exclude males in this study, a tail sample was taken, the DNA was extracted and a polymerase chain reaction (PCR) for sex-determining region Y (*SRY*) was performed as previously described (Hummitzsch *et al.* 2013). For histology and immunohistochemistry, one ovary from each pair was weighed and processed for further analysis, whereas for RNA analysis, the corresponding ovary was snap-frozen on dry ice and stored at −80°C for subsequent RNA extraction.

Ovaries of known gestational age

An additional group of fetal ovaries was derived from another study in which the age of the fetus was known. The experimental design of the cattle trial from which these fetal ovaries were obtained has been described previously (Copping *et al.* 2014). Briefly, the influence of diet on development *in utero* was assessed on Santa Gertrudis (*Bos taurus* × *Bos indicus*) heifers divided into four groups according to different dietary protocols based on a two-by-two factorial crossover design. The heifers were randomly assigned to either a high (H = 14% crude protein, (CP)) or low (L = 7% CP) protein diet 60 days before conception to 23 days postconception (dpc; periconception treatment). This diet was individually fed in stalls and straw (5% crude protein) was available ad libitum. The ration was as isocaloric as possible in the ruminant and supplemented with a commercial vitamin and mineral preparation (Ridley Agriproducts). The heifers were synchronously artificially inseminated to a single bull. At 23 dpc, half of each nutritional treatment group was swapped to the alternative postconception treatment, high or low. At the end of the first trimester (98 dpc), heifers were culled and the fetuses and placentae were collected. The fetuses were sexed and the fetal gonads were excised and weighed. One gonad from each fetus was processed for histology and two ovaries from each of the four groups were analysed by morphometry.

Histology

Fetal ovaries from the abattoir ($n = 27$) and the ovaries of known gestational age ($n = 8$) were fixed in 4% paraformaldehyde (Merck Pty Ltd) in 0.1 M phosphate buffer (pH 7.4) and embedded in paraffin using a Leica EG 1140H (Leica Microsystems). Serial sections of 6 µm were prepared using a CM1850 V2.2 Leica microtome (Leica Microsystems), mounted on Superfrost glass slides (HD Scientific Supplies) and stored at room temperature until used for haematoxylin–eosin staining and immunohistochemistry.

Sample grouping

Abattoir samples were sorted into five groups based on histological morphology, as follows: Stage I, ovigerous cord formation (the period when the ovigerous cords are formed ($n = 7$)); Stage II, ovigerous cord breakdown (the period when most of the ovigerous cords have broken down ($n = 4$)); Stage III, follicle formation (the period when most of primordial and primary follicles have formed but the cords are still open to the ovarian surface ($n = 3$)); Stage IV, ovarian surface epithelium formation (the time point when the ovarian surface epithelium is completely formed ($n = 8$)) and Stage V, tunica albuginea formation (the time point when tunica albuginea is formed ($n = 5$)). Additionally, the age of each fetus was estimated from the CRL ($y = -0.0103x^2 + 3.4332x + 36.08$, where y is age in days and x is CRL in cm and calculated from the method of Russe (1983)).

Immunohistochemistry

An indirect immunofluorescence method was used for dual localisation of Ki67 and collagen type I (Irving-Rodgers *et al.* 2002). Paraffin-embedded sections from different ovaries ($n = 35$ animals) were dewaxed then subjected to a pressure-cooker antigen retrieval method for 20 min (2100 retriever; Prestige Medical Ltd) in 10 mM Tris–ethylenediamine tetraacetic acid (EDTA) buffer (pH 9.0). The primary antibodies

used were mouse anti-human Ki67 (1 : 800; M7240/MIB-1; DAKO Australia Pty Ltd) to identify proliferating cells in combination with rabbit anti-human collagen type I (1 : 400; 20 μg mL^{-1}; ab34710; Abcam) to mark the stroma. Secondary antibodies were donkey anti-mouse IgG conjugated to Cy3 (1 : 100; 715 166 151) and Biotin–(SP)-conjugated AffiniPure donkey anti-rabbit IgG (1 : 100; 711 066 152) followed by dichlorotriazinylamino fluorescein (DTAF)-conjugated streptavidin (1 : 100; 016 010 084). All secondary antibodies and conjugated streptavidin were from Jackson ImmunoResearch Laboratories Inc. Cell nuclei were counterstained with 4',6'-diamidino-2-phenylindole dihydrochloride (DAPI) solution (Molecular Probes). The bovine adult ovary was used as a positive control whereas nonimmune mouse and rabbit sera (Sigma-Aldrich) were used as negative controls. All sections were photographed with an Olympus BX51 microscope with an epifluorescence attachment and a Spot RT digital camera (Diagnostic Instruments) at a magnification of 40×.

Morphometric analyses

The largest cross-section from each ovary, determined by haematoxylin–eosin staining for every 10th section, was examined using NPD.view2 software (Hamamatsu Photon). Using the ImageJ software (Schindelin *et al.* 2012), images of the cortex at 40× magnification were taken randomly with a single image dimension set at 1600 × 1200 pixels (0.06 mm^2). Each image represented a field of view that was used for morphometric analysis in this study. The total number of fields of view to be examined for each analysis was first determined by examining the coefficient of variation (CV) of 3–40 fields of view. For measuring the stromal area, the following steps were performed (Fig. 1). First, the total cortical area was identified, saved as a region of interest (tissue area) and its area measured. Next, the stromal area in the cortex was identified based on positive collagen type I staining (Fig. 2). To calculate the proportion of stroma in the cortex (volume density) and total stromal volume, the following calculations were applied and all calculations used equations that are listed in Table 1. The ovarian volume (V_{ovary}) was estimated using the ovarian weight, assuming a density of 1 g cm^{-3}. Then, the proportion of stroma in the cortex ($V_{v[stroma]}$) and the total stromal volume (V_{stroma}) were calculated using the equations shown in Table 1. The number of proliferating stromal cells (Ki67 positive) and all stromal cells (DAPI positive) in a field of view were counted using the multipoint and find maxima tool with adjusted noise tolerance (ImageJ). Nuclei, which were not detected by the threshold, were added manually using the multipoint tool. Results of proliferating cells are presented as a proliferation index (*PI*) and as a numerical density (N_{dp}/N_d) in the stromal area using the equations shown in Table 1.

RNA extraction and cDNA synthesis

RNA was extracted from the whole fetal ovary using 1 mL Trizol (Thermo Fisher Scientific) with 0.5 g of ceramic beads in homogenisation tubes using the Mo Bio Powerlyser 24 (Mo Bio Laboratories Inc.) and 200 μL chloroform (RNase-free) according to the manufacturer's instructions. The RNA concentration was determined using a Nanodrop spectrophotometer

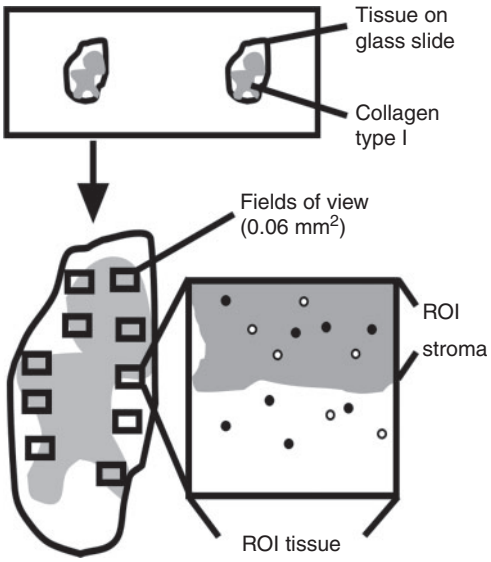

Fig. 1. Schematic diagram of the procedure for determining the stromal areas and proliferating cells in fetal ovarian tissues. For immunohistochemistry and subsequent analysis by ImageJ, the largest cross-section of each fetal ovary was used and 20–40 fields of view (each 0.06 mm^2) were randomly chosen from each section. Fluorescence staining for collagen type I was used to distinguish between stromal and non-stromal areas and Ki67 was used to mark any proliferating cells in the ovarian tissue. In each photograph the total ovarian tissue was marked as region of interest (ROI) tissue and measured. The stromal area, marked by collagen type I fibres (shaded areas), was identified as ROI stroma and measured. Ki67-positive cells (black dots) and DAPI-positive cells (white dots) were counted in stromal areas.

(NanoDrop 1000 3.7.1; Nanodrop Technologies) based on the 260λ (wavelength) absorbance. All samples which had a 260 : 280λ absorbance ratio >1.8 were used and subsequently treated with DNase I (Promega/Life Technologies Australia Pty Ltd). Complementary DNA was then synthesised from 200 ng of DNase-treated RNA using 250 ng μL^{-1} random hexamers (Geneworks) and 200 U Superscript Reverse Transcriptase III (Thermo Fisher Scientific) as previously described (Matti *et al.* 2010). For a negative control, diethyl pyrocarbonate (DEPC)-treated water instead of the Superscript Reverse Transcriptase III was added.

Quantitative real-time PCR

To conduct quantitative real-time PCR (qPCR), primers were designed against the published reference RNA sequences (Table 2) using Primer3 plus (Rozen and Skaletsky 2000) and Net primer (PREMIER Biosoft) software. To test the combination of primers, the cDNA was diluted to five different concentrations from 1 : 4 to 1 : 1000 to generate a standard curve of cycle threshold (Ct) versus concentrations. Primer combinations that showed a single sharp peak and achieved an amplification efficiency of 0.9–1.1 and an R^2 value ≥ 0.98 were used for further analysis.

Quantitative PCR was carried out using a Rotor-Gene 6000 series 1.7 thermal cycler (Qiagen GmbH) in duplicate at 95°C

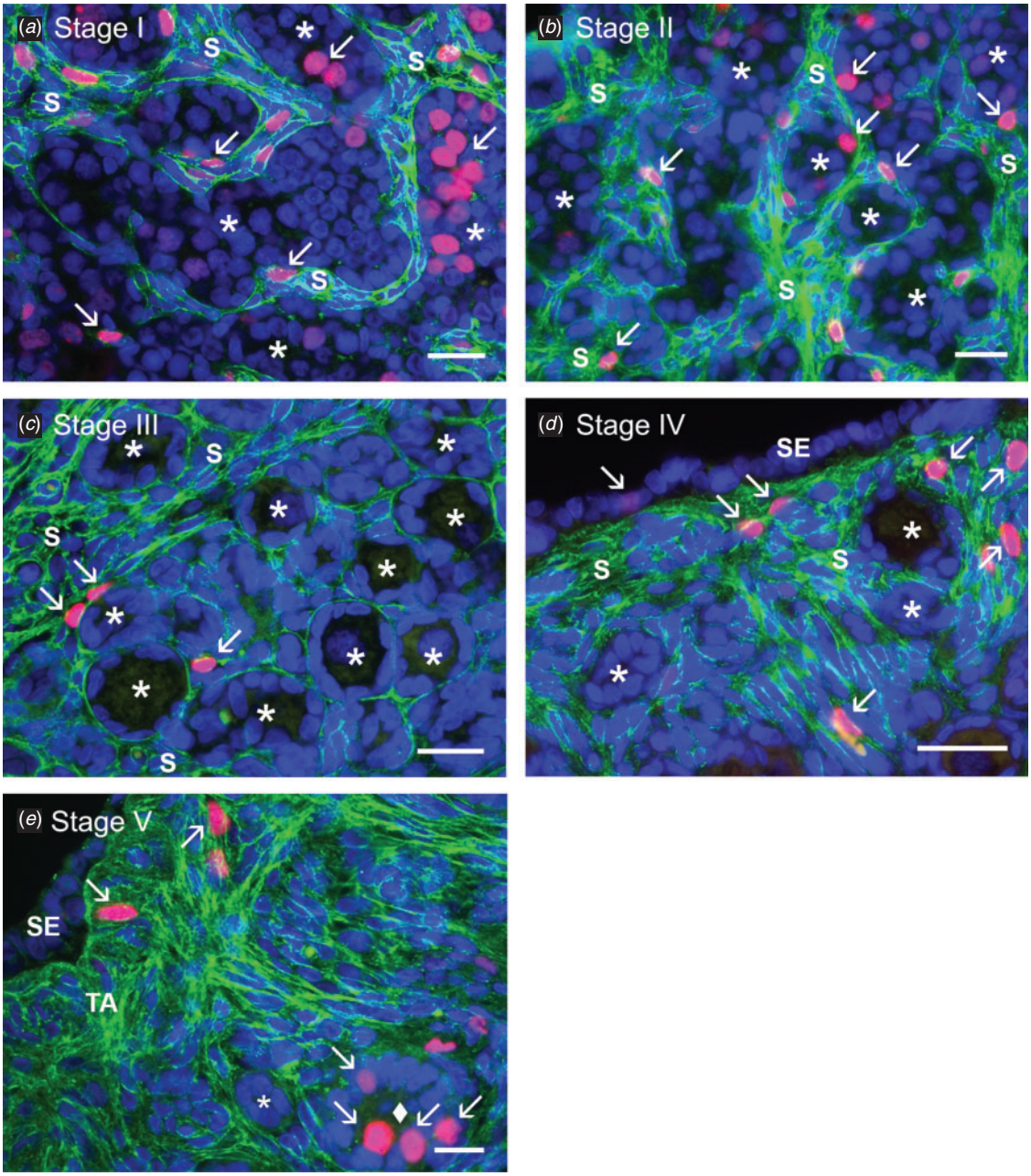

Fig. 2. Stromal distribution and proliferation in fetal ovaries from different developmental stages. Representative photographs from (*a*) Stage I (ovigerous cord formation), (*b*) Stage II (ovigerous cord breakdown), (*c*) Stage III (follicle formation), (*d*) Stage IV (ovarian surface epithelium formation) and (*e*) Stage V (tunica albuginea formation) of fetal ovarian development showing stroma (S), ovigerous cords–primordial follicles (marked with asterisks), surface epithelium (SE), tunica albuginea (TA) and a preantral follicle (marked with diamond). The stroma was identified based on the expression of collagen type I, which is a stromal marker. Collagen type I (green) is combined with the proliferation marker Ki67 (red, marked with arrows). Nuclei are counterstained with DAPI. Scale bar = 25 μm.

for 15 s then 60°C for 60 s for 40 cycles. Amplification of cDNA dilutions were prepared in 10 μL reactions containing 2 μL of the 1 : 20 cDNA dilution, 5 μL Power SYBR Green PCR Master Mix (Applied Biosystems), 0.2 μL each of forward and reserve primers (Geneworks; Table 2) for the target genes and 2.6 μL of DEPC-treated water. Ct values were determined using the Rotor-Gene 6000 software (Q series; Qiagen GmbH) at a threshold of 0.05 normalised fluorescence units. Gene expression was determined by the mean of $2^{-\Delta Ct}$, where ΔCt represents the target gene Ct – glyceraldehyde-3-phosphate dehydrogenase (*GAPDH*) Ct. *GAPDH* was used as a housekeeping gene because it is stably expressed in bovine adult ovarian tissues

Table 1. List of equations for morphometric analyses

A_{cortex}, cortical area in each image; A_{ovary}, ovarian area in each image; A_{stroma}, stromal area in each image; $A_{totalstroma}$, total analysed stromal area; $N_{pstroma}$, total number of proliferating cells in all analysed images of the stroma; N_{stroma}, total number of cells in all analysed images of the stroma; V_{ovary}, ovarian volume

Parameter	Equation	Units
Proportion of cortex in the ovary or cortical volume density ($V_{v[cortical]}$)	$V_{v[cortical]} = A_{cortex} / A_{ovary}$	%
Cortical volume (V_{cortex})	$V_{cortex} = V_{v[cortical]} \times V_{ovary}$	mm^3
Proportion of stroma in cortex or volume density of stroma in the ovarian cortex ($V_{v[stroma]}$)	$V_{v[stroma]} = A_{stroma} / A_{cortex}$	%
Cortical stromal volume (V_{stroma})	$V_{stroma} = V_{v[stroma]} \times V_{cortex}$	mm^3
Proliferation index in the cortical stroma (*PI*)	$PI = N_{pstroma} / N_{stroma}$	%
Numerical density of proliferating cells in the stroma (N_{dp})	$N_{dp} = N_{pstroma} / A_{totalstroma}$	$N\,mm^{-2}$
Numerical density of all cells in the stroma (N_d)	$N_d = N_{stroma} / A_{totalstroma}$	$N\,mm^{-2}$

Table 2. List of genes and primers used for quantitative real-time PCR

Gene name	Gene symbol	Primers (5′→3′)	Genebank accession number	Size (bp)
Glyceraldehyde-3-phosphate dehydrogenase	*GAPDH*	F: ACCACTTTGGCATCGTGGAG R: GGGCCATCCACAGTCTTCTG	NM_001034034.2	76
Osteoglycin	*OGN*	F: TGCAAGGCTAATGACACCAG R: GATGTTTTCCCAGGATGACG	NM_173946.2	85
Lumican	*LUM*	F: TTCAAAGCATTCGCCAAAATG R: CCGCCAATTAATGCCAAGAG	NM_173934.1	62
Asporin	*ASPN*	F: AAGGACATGGAAGACGAAGG R: GGGAAGAAGGGGTTAATTGG	NM_001034309.2	80
Fibromodulin	*FMOD*	F: AGGTGGGCAAGAAGGTTTTC R: TCTGGTTGTGGTCAAGATGG	NM_174058.2	129
Biglycan	*BGN*	F: CACCTTGGTGATGTTGTTGG R: TCTCGTCCGCTACTCCAAGT	NM_178318.4	202
Collagen type VI α1 chain	*COL6A1*	F: CAAGGATGTCTTTGGCTTGG R: AGAAGCTCGGCGTAGTTTTC	NM_001143865.1	120
Collagen type VI α2 chain	*COL6A2*	F: TCAAAGAGGCCGTCAAGAAC R: TGAGCTTGTTGTAGGCGAAC	NM_001075126.1	84
Collagen type VI α3 chain	*COL6A3*	F: TCAATACCTACCCCAGCAAGA R: GACCGCATCTAGGGACTTACC	XM_005197965.3	200
Collagen type I α2 chain	*COL1A2*	F: TTGAAGGAGTAACCACCAAGG R: TGTCCAAAGGTGCAATATCAA	NM_174520.2	321
Fibronectin	*FN1*	F: CGACGGCATCACTTACAATG R: CGACGGCATCACTTACAATG	NM_001163778.1	118
Fibronectin extra domain A	*FN1-EDA*	F: CCTGTTACTGGTTACAGAGTG R: AGTGAGCTGAACATTGGG	AF 260303	550
Fibronectin extra domain B	*FN1-EDB*	F: GCCGATCAGAGTTCCTGCACC R: GAGCCCAGGTGACACGCATAG	AF 260304	456
Fibronectin V region	*FN1-V*	F: CTGAAGAACAATCAGAAGAG R: CCACTATGATGTTGTAGGTG	AF 260305	600
Lectin, galactoside-binding soluble 1 (galectin 1)	*LGALS1*	F: AATCATGGCTTGTGGTCTGG R: AGGTTGTTGTCGTCTTTGCC	NM_175782.1	129
Regulator of G-protein signalling 5	*RGS5*	F: GCCATTGACCTTGTCATTCC R: TTGTTCTGCAGGAGCTTGTC	NM_001034707.2	119
Fibulin-1	*FBLN1*	F: GCAGCGCAGCCAAGTCAT R: AGATATGTCTGGGTGCTACAAACG	NM_001098029.1	66
Fibulin-2	*FBLN2*	F: TGGCACTCACGATTGTAACC R: GTTGATGTCCACGCATTTCC	XM_589271.8	130
Fibulin-5	*FBLN5*	F: TGCAACTGAGAATCCCTGTG R: GCATTCGTCCATATCACTGC	NM_001014946	121

Table 3. Characteristics of developmental stages (I to V) of bovine fetal ovaries from the abattoir collection
Data are mean ± s.e.m. One-way ANOVA with post hoc Tuckey's tests were used to analyse data. [a,b,c,d]Values within a row with different superscripts indicate significant differences ($P < 0.05$)

Parameter	Developmental stage				
	I	II	III	IV	V
Gestational age (days)[A,B]	79 ± 6^{a}	127 ± 6^{b}	173 ± 12^{c}	234 ± 9^{d}	264 ± 6^{d}
Time from previous stage (days)		48	46	61	30
Weight (mg)[B]	17.9 ± 5.1^{a}	49.2 ± 7.9^{b}	113.5 ± 33.6^{bc}	245.8 ± 62.9^{cd}	475.3 ± 22.6^{c}
Fold change in weight from previous stage		2.7	2.3	2.2	1.9
Total cortical volume (mm^3)[B]	10.3 ± 3.0^{a}	30.1 ± 4.8^{b}	70.7 ± 27.4^{bc}	65.5 ± 9.0^{bcd}	142.1 ± 37.5^{cd}
Fold change in cortical volume from previous stage		2.9	2.3	0.9	2.2
Cortical volume density (%)	56.9 ± 3.0^{a}	61.7 ± 6.7^{a}	59.7 ± 9.1^{ab}	33.2 ± 5.5^{bc}	29.5 ± 7.0^{c}
Total medullar volume (mm^3)[B,C]	7.7 ± 2.1^{a}	19.0 ± 4.5^{ab}	42.8 ± 9.5^{bc}	180.3 ± 57.9^{cd}	333.1 ± 34.8^{d}
Fold change in medullar volume from previous stage		2.5	2.5	4.2	1.8
Total cortical stromal volume (mm^3)[B]	3.3 ± 0.8^{a}	12.9 ± 1.9^{b}	43.4 ± 20.1^{bc}	49.6 ± 7.3^{cd}	112.7 ± 28.1^{cd}
Fold change in cortical stroma from previous stage		3.9	3.4	1.1	2.3

[A]Estimated from the CRL (Russe 1983).
[B]Statistical analysis was conducted using log-transformed data.
[C]Calculated from total cortical volume and percentage of medullar area.

(Berisha *et al.* 2002) and showed stable expression in our samples.

Statistical analyses

All statistical analyses were carried out using Microsoft Office Excel 2010 and GraphPad Prism Version 6.00 (GraphPad Software Inc.). All data that were not normally distributed or showed significantly different standard deviations between groups were first log-transformed. The morphometric and $2^{-\Delta Ct}$ data for each fetal ovarian sample were compared using ANOVA with Tukey's *post-hoc* test. A value of $P < 0.05$ was considered to be significant. For testing the association between expression levels of each gene throughout development, correlation coefficients were determined using the Spearman correlation coefficient. After correlation values between genes were identified, a network graph was plotted using the qgraph R package (Epskamp *et al.* 2012) and illustrated using an adjacent matrix plot.

Results

Classification of ovaries

As we have observed previously (Hummitzsch *et al.* 2013), there was variation in the developmental stage of ovaries from fetuses of the same crown–rump length, particularly at early stages. We therefore devised a classification system based upon five identifiable stages of development of the cortex commencing with ovigerous cord formation (Stage I), ovigerous cord breakdown (Stage II), follicle formation (Stage III), surface epithelium formation (Stage IV) and tunica albuginea formation (Stage V) as illustrated in Fig. 2 and subsequently analysed data from the abattoir collection using this classification system.

Determination of total number of fields of view

Using the ovaries from our abattoir collections we first determined the optimum number of total fields of view required for the morphometric measurements of the proportion of stroma in the cortex and the proportion of proliferating stromal cells in the ovarian cortex. A CV analysis was conducted from 3 up to 40 fields of view photographed at 40× magnification accounting for 0.06 mm^2 (Fig. S1, available as Supplementary Material to this paper). For fetuses with a CRL <30 cm, the CV of the volume density of stroma (Fig. S1*a–c*) and the proportion of proliferating stromal cells in the ovarian cortex (Fig. S1*g–i*) was relatively variable until nine fields of view and then remained similar until 20 fields of view. However, for fetuses with CRL of 39 cm the CV of the proportion of stroma in the cortex (Fig. S1*d*) and the proportion of proliferating stromal cells in the ovarian cortex (Fig. S1*j*) were similar for almost all numbers of fields of view. For fetuses with CRL >50 cm, the parameters were highly variable from 3 to 20 fields of view (Fig. S1*e*, *f*, *k*, *l*) and then stabilised from 20 to 40 fields of view. Thus, for morphometric quantitation of fetuses with a CRL of <50 cm we assessed 10 fields of view and for fetuses with a CRL of >50 cm we assessed 20 fields of view.

Ovary changes in Stages I to V

Details of the ovaries and fetuses of each stage from our abattoir collection are presented in Table 3. With advancing stages the fetuses were older and the ovaries became significantly heavier and they had more cortex and medulla, but proportionally less cortex relative to medulla in the last two stages of development (Table 3). We calculated the time to transit from one stage to the next and fold changes between each stage in weight, cortical volume and medullary volume (Table 3). The transition time between Stages I and II, II and III, III and IV and IV and V were 48, 46, 61 and 30 days respectively (Table 3); thus, the duration of development before Stage III was 94 (48 + 46) days and after Stage III was 91 (61 + 30) days. From Stages I to III versus Stages III to V the fold changes in weight were 6.2 and 4.2, the fold changes in cortical volume were 6.7 and 2.0 and the fold changes in medullary volume were 6.3 and 7.6 respectively

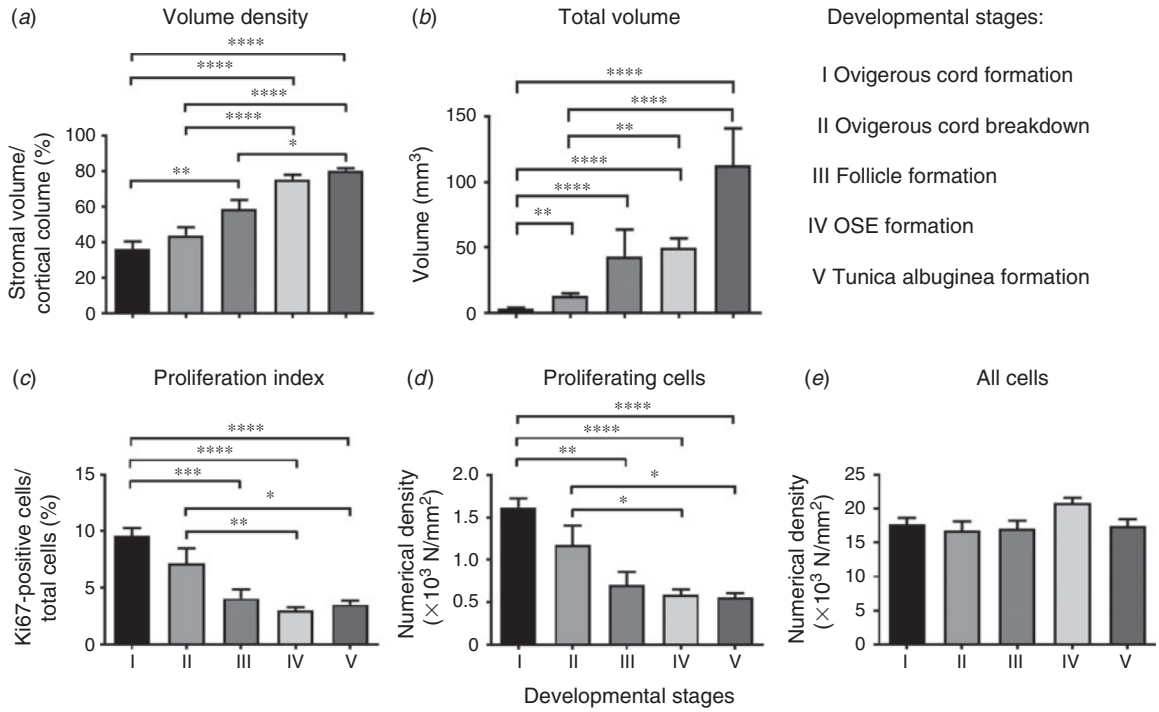

Fig. 3. Morphometric analyses of the stroma during bovine fetal ovarian development. Data are presented as mean ± s.e.m. Samples were grouped into five stages of ovarian development based on their histological morphology: ovigerous cord formation ($n = 7$, Stage I), ovigerous cord breakdown ($n = 4$, Stage II), follicle formation ($n = 3$, Stage III), ovarian surface epithelium (OSE) formation ($n = 8$, Stage IV) and tunica albuginea formation ($n = 5$, Stage V). (*a*) Volume density represents the proportion of stroma in the cortex, (*b*) total volume represents the total stromal volume in the ovarian cortex, (*c*) proliferation index represents the ratio between total proliferating and all cells in the cortical stroma, (*d*) proliferating cells represents the numerical density of proliferating cells in the cortical stroma and (*e*) all cells represents the numerical density of all cells in the cortical stroma. One-way ANOVA with post hoc Tuckey's tests were used to analyse the data. *$P < 0.05$, **$P < 0.01$, ***$P < 0.001$, ****$P < 0.0001$.

(calculated from Table 3). Thus, after Stage III when follicles formed, the expansion of the cortex slowed but the medulla continued to expand at its previous rate, leading to proportionally more medulla. From 79 to 264 days of gestation the ovarian volume increased 26.5 fold (17.9 to 475.3 mm^3), the cortex increased 13.8 fold in volume (10.3 to 142.1 mm^3) and the medulla increased 34.1 fold in volume (3.3 to 112.7 mm^3).

Morphometric characteristics of fetal ovarian stroma

During ovigerous cord formation at Stage I (Fig. 2*a*), the stroma containing many Ki67-positive cells formed branches between ovigerous cords (Fig. 3*c*, *d*). At this stage the ovigerous cords contained oogonia, undergoing mitosis as shown by colocalisation with the proliferation marker Ki67 (Fig. 2*a*). The proportion of stroma in the ovarian cortex increased during ovigerous cord breakdown at Stage II (Fig. 3*a*, *b*), although it was not statistically significant. Ki67-positive cells were observed in the stromal area and in the partitioned ovigerous cords (Fig. 2*b*). In the stromal area, the total number of Ki67-positive cells was lower than during Stage I (Fig. 3*c*, *d*); however, the difference was not statistically significant. During follicle formation at Stage III (Fig. 2*c*), the proportion of stroma in the ovarian cortex had increased further (Fig. 3*a*, *b*). The stroma now surrounded the primordial follicles, which were first formed at the inner cortex adjacent to the medulla. Proliferating cells were observed in the stroma but not in primordial follicles (Fig. 2*c*); however, the total number of Ki67-positive cells in stroma were lower than during Stage II (Fig. 3*c*, *d*), although the difference was not statistically significant. During the formation of surface epithelium at Stage IV (Fig. 2*d*), the ovary had more stroma underneath the ovarian surface. At this stage Ki67-positive cells localised in the stroma as well as the ovarian surface. Tunica albuginea formation at Stage V was characterised by bundles of thick collagen type I fibres underneath the ovarian surface epithelium (Fig. 2*e*). At this stage stromal cells and some granulosa cells in growing follicles were positive for Ki67.

We quantitatively measured the proportion of stroma in the cortex and the total volume of the stroma in the cortex (Fig. 3) and both were significantly increased during ovarian development ($P < 0.05$; Fig. 3*a*, *b*). Interestingly, the cell proliferation index of the stroma in the ovarian cortex significantly declined during ovarian development (Fig. 3*c*). The numerical density of proliferating cells also significantly declined in the cortical stroma throughout gestation (Fig. 3*d*). However, the numerical density of cortical stromal cells was stable during ovarian development (Fig. 3*e*), suggesting that the increase in stromal volume during gestation was not affected by an increase in extracellular space in the cortical stroma.

Table 4. Morphometric analyses of the cortical stroma in bovine fetal ovaries from the trial at Day 98 of gestation
Data are mean ± s.e.m. ($n = 8$)

Characteristic	Value
Weight (mg)	26.5 ± 1.1
Total volume cortical stroma (mm^3)	3.9 ± 0.2
Proportion of stroma in the cortex (%)	26.1 ± 0.1
Proliferation index of cortical stroma (%)	7.3 ± 0.5
Numerical density of proliferating cells in cortical stroma ($N\,mm^{-2}$)	1340 ± 77
Numerical density of cortical stromal cells ($N\,mm^{-2}$)	18 737 ± 607

To assess if our morphometric analyses used for the abattoir collection were adequate, we analysed fetal ovarian samples from the trial collected on Day 98 of gestation. Using the CRL, age was estimated by the method of Russe (1983) to be 95.3 ± 1.2 days, which is in very good agreement with the known age of 98 days. During this time of gestation, the stroma occupied 26.1 ± 0.1 % of the cortex and was 3.9 ± 0.2 mm^3 in total volume. The proliferation index of the cortical stroma was 7.3 ± 0.5 %, the numerical density of the proliferating stromal cells in the cortex was 1340 ± 77 cells mm^{-2} and the numerical density of all the stromal cells was 18 737 ± 607 cells mm^{-2} (Table 4).

Gene expression

We analysed the mRNA expression of genes that are specifically expressed in the stroma of many adult tissues, including the ovary. The mRNA expression of osteoglycin (*OGN*), lumican (*LUM*), asporin (*ASPN*), collagen type VI A1 (*COL6A1*), *COL6A2*, *COL6A3*, fibronectin (*FN1*), regulator of G-protein signalling 5 (*RGS5*) and fibulin 5 (*FBLN5*) in fetal ovaries significantly increased in Stages IV and V of development (Fig. 4*a–c*, *g–j*, *o*, *r*) relative to earlier stages. We also analysed the mRNA expression of another three *FN1* splice variants (FN1 extra domain A (*FN1-EDA*), FN1 extra domain B (*FN1-EDB*) and FN1 variable (*FN1-V*)), which have three different additional domains. Our results showed that *FN1-EDA*, *FN1-EDB* and *FN1-V* were also significantly increased late in development (Fig. 4*k–m*). The expression of fibromodulin (*FMOD*), biglycan (*BGN*), *COL1A2*, *FBLN1*, *FBLN2* and Lectin galactoside-binding soluble 1 (galectin 1) *(LGALS1)* did not show any significant differences across stages of ovarian development (Fig. 4*d–f*, *n*, *p*, *q*).

Correlation analyses

To analyse the correlations between the 18 genes of interest and additionally with gestational age (Table 5), we generated the Spearman correlation matrix from the Ct values of all genes. After correlation values between genes were identified, a network graph was plotted using the qgraph R package (Epskamp *et al.* 2012) to plot an adjacent matrix (Fig. 5) and some examples of these are correlations as shown in Fig. 6. *OGN*, *LUM*, *ASPN*, *BGN*, *COL6A1*, *COL6A2*, *COLA3*, *COL1A2*, *FN1*, *FN1-EDA*, *FN1-EDB*, *FN1-V*, *RGS5*, *FBLN1* and *FBLN5* were all strongly positively associated with each other ($r > 0.6$). In addition, *FMOD* had strong positive correlations ($r > 0.6$) with *BGN*, *COL6A1*, *COL6A2*, *COLA3*, *COL1A2*, *FN1*, *FN1-EDA*, *FN1-EDB*, *FN1-V* and *LGALS1*. *FBLN2* and *LGALS1* showed weaker positive relationships to other genes ($r < 0.6$). Gestational age had strong positive correlations ($r > 0.6$) with *FBLN5*, *LUM*, *RGS5*, *ASPN*, *OGN*, *FN1-EDB*, *COL6A3*, *COL6A2*, *COLA1*, *FN1-V*, *FN1-EDA*, *COL1A2* and *FBLN1*, but had weaker positive correlations ($r < 0.6$) with *FN1*, *BGN*, *LGALS1* and *FMOD* (Table 5). Interestingly, *FBLN2* had a weak negative correlation with gestational age (Table 5).

Discussion

In this study we conducted morphometric analyses of the developing bovine fetal ovary, focusing on cortical stroma. We were able to identify the stroma by immunostaining of the stromal extracellular matrix collagen type I. We optimised our morphometric sampling regime and also examined ovaries of a known stage of gestation. Across gestation we measured the total volume and relative proportions of cortex and medulla, the proportion and total volume of stroma in the cortex and the numerical and proliferation index of cells in the stroma of the cortex. We also examined the expression of 18 genes that had previously been reported as relevant to stroma in other organs. We believe this is one of the first critical studies of the development of ovarian stroma.

Collagen type I is an extracellular matrix of stroma that has been localised in the stroma of fetal bovine (Hummitzsch *et al.* 2013) and rat ovaries (Paranko 1987), as well as adult bovine (Figueiredo *et al.* 1995), mouse (Berkholtz *et al.* 2006) and human (Lind *et al.* 2006) ovaries. Collagen type I was observed at all stages of fetal bovine ovary development by immunostaining but the intensity of immunostaining increased qualitatively throughout development. This suggests that greater deposition of collagen type I occurs during fetal development, leading to a stiffer stromal matrix.

An earlier morphometric study examining the bovine fetal ovary has been conducted but over a shorter period of time than our study. From their results we calculated that the ovary volume increased 4.2 fold in volume (35 to 148 mm^3), the cortex increased 2.8 fold in volume (21.9 to 62.4 mm^3) and the medulla increased 6.5 fold (13.1 to 85.6 mm^3) from 3 to 7 months of gestation (Santos *et al.* 2013). Our measurements are in agreement with theirs where, during Stages I to III (taking 94 days) versus Stages III to V (taking 91 days) the changes in ovarian weight were 6.2 and 4.2 fold, in medullary volume were 6.3 and 7.6 fold and in cortical volume were 6.7 and 2.0 fold respectively. Our values are higher than theirs as our study was over a longer time frame. Our results also show that throughout gestation the medulla expanded substantially more (34.1 fold) than the cortex (13.8 fold) did and that the rate of expansion of the cortex declined past Stage III when follicles were formed. What drives the continued expansion of the medulla is not known, nor why this would continue.

The numerical density (cells per area or volume) of cells in the cortical stroma, however, did not change across gestation. Assuming that the sizes of the stromal cells did not change, and there was no observable evidence that they did, then the

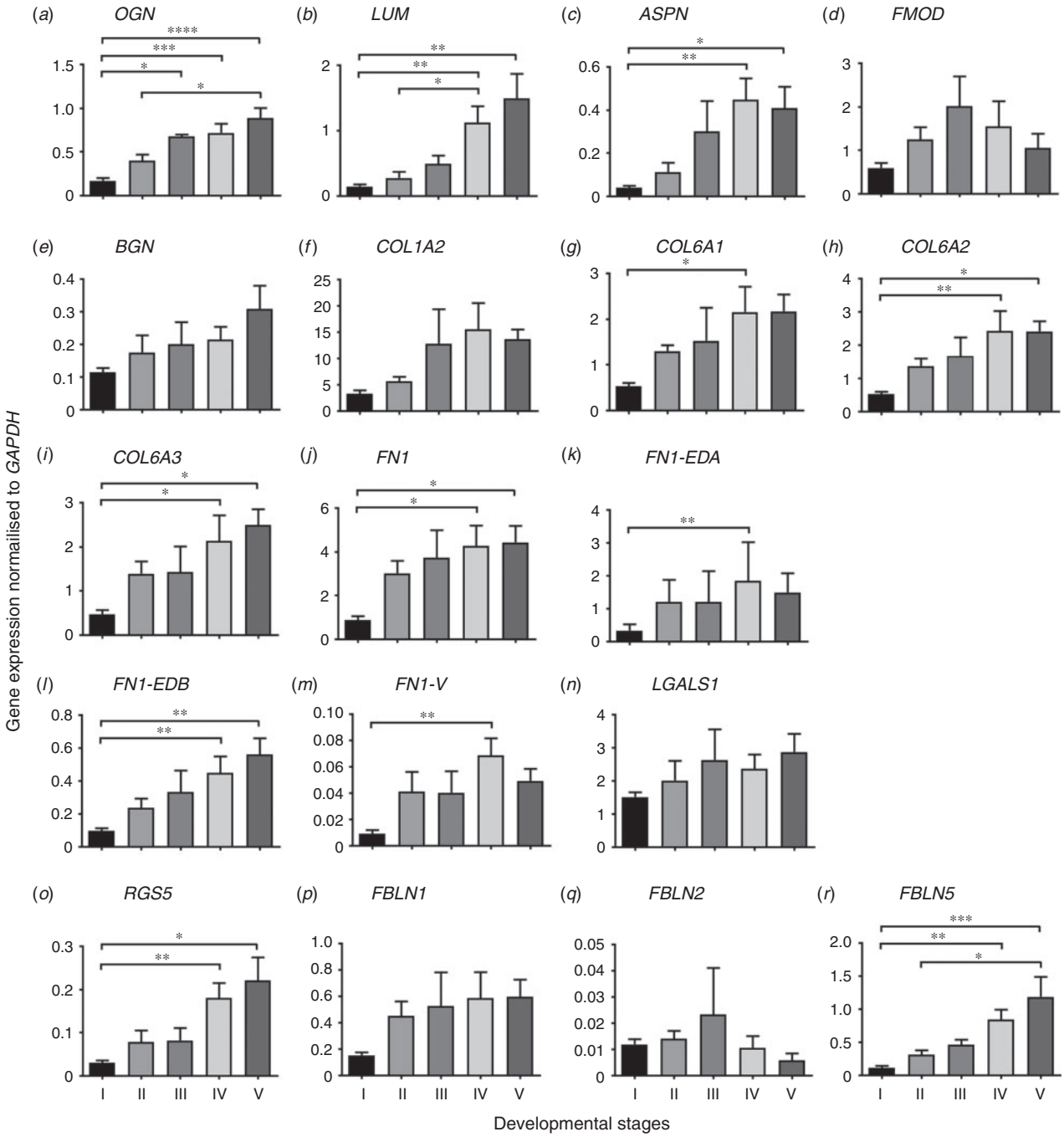

Fig. 4. Differential mRNA expression levels of genes in whole bovine fetal ovaries. One ovary from each pair was used for mRNA analysis ($n = 27$ pairs). Data are presented as mean ± s.e.m. (normalised to *GAPDH*). Samples were grouped into five stages of ovarian development based on their histological morphology: ovigerous cord formation ($n = 7$, Stage I), ovigerous cord breakdown ($n = 4$, Stage II), follicle formation ($n = 3$, Stage III), surface epithelium formation ($n = 8$, Stage IV) and tunica albuginea formation ($n = 5$, Stage V). One-way ANOVA with post hoc Tuckey's tests were used to analyse the data. *$P < 0.05$, **$P < 0.01$, ***$P < 0.001$, ****$P < 0.0001$.

proportion of extracellular space in the cortical stroma was constant across gestation. This is different from what is known to happen in the tunica albuginea, which has a significantly lower cell numerical density than cortical stroma and has proportionally more extracellular space rich in extracellular matrix containing at least collagens, versican, fibronectin, decorin (Hummitzsch *et al.* 2013), latent transforming growth factor β-binding protein 2 and fibrillin 1 (Prodoehl *et al.* 2009). Thus, as also observed in the human fetal ovary from 20 to 25 weeks of gestational age (Sforza *et al.* 1993), there was an

Table 5. Spearman correlation coefficients (*r*) of mRNA expression levels of stroma-related genes and gestational age (*n* = 27)

*$P < 0.05$, **$P < 0.01$, ***$P < 0.001$, ****$P < 0.0001$

	LGALS1	*OGN*	*RGS5*	*FBLN5*	*ASPN*	*COL1A2*	*COL6A1*	*COL6A2*	*COL6A3*	*FBLN1*	*FBLN2*	*FN1-EDA*	*FN1-EDB*	*FN1-V*	*FN1*	*LUM*	*FMOD*	*BGN*
LGALS1	–																	
OGN	0.646***	–																
RGS5	0.587**	0.769****	–															
FBLN5	0.522*	0.897****	0.834****	–														
ASPN	0.480*	0.786****	0.898****	0.877****	–													
COL1A2	0.515**	0.792****	0.741****	0.876****	0.859****	–												
COL6A1	0.477*	0.759****	0.85****	0.845****	0.887****	0.910****	–											
COL6A2	0.477*	0.766****	0.868****	0.853****	0.891****	0.904****	0.979****	–										
COL6A3	0.585**	0.809****	0.86****	0.886****	0.856****	0.896****	0.967****	0.959****	–									
FBLN1	0.573**	0.628***	0.801****	0.675***	0.732***	0.744****	0.847****	0.863****	0.889****	–								
FBLN2	0.072	0.077	0.033	0.049	0.170	0.226	0.322	0.273	0.272	0.386*	–							
FN1-EDA	0.574**	0.737****	0.859****	0.835****	0.881****	0.889****	0.941****	0.953****	0.950****	0.884****	0.337	–						
FN1-EDB	0.582**	0.820****	0.872****	0.911****	0.869****	0.919****	0.92****	0.944****	0.949****	0.839****	0.157	0.935****	–					
FN1-V	0.592**	0.740****	0.864****	0.831****	0.860****	0.832****	0.867****	0.889****	0.892****	0.827****	0.264	0.966****	0.905****	–				
FN1	0.554**	0.781****	0.630***	0.797****	0.694****	0.775****	0.734****	0.730****	0.758****	0.634***	0.096	0.769****	0.739****	0.754****	–			
LUM	0.436*	0.869****	0.806****	0.914****	0.877****	0.823****	0.833****	0.841****	0.856****	0.694****	0.079	0.824****	0.847****	0.813****	0.684****	–		
FMOD	0.609***	0.518**	0.520**	0.491**	0.522**	0.671***	0.674***	0.708****	0.725****	0.814****	0.434*	0.759****	0.698****	0.695****	0.604***	0.485*	–	
BGN	0.594**	0.752****	0.658***	0.747****	0.697****	0.817****	0.801****	0.785****	0.817****	0.737****	0.312	0.804****	0.828****	0.79****	0.763****	0.745****	0.699****	–
Gestational age	0.416*	0.818****	0.876****	0.895****	0.868****	0.720****	0.750****	0.765****	0.776****	0.600***	0.217	0.724****	0.808****	0.727****	0.571**	0.877****	0.321	0.563**

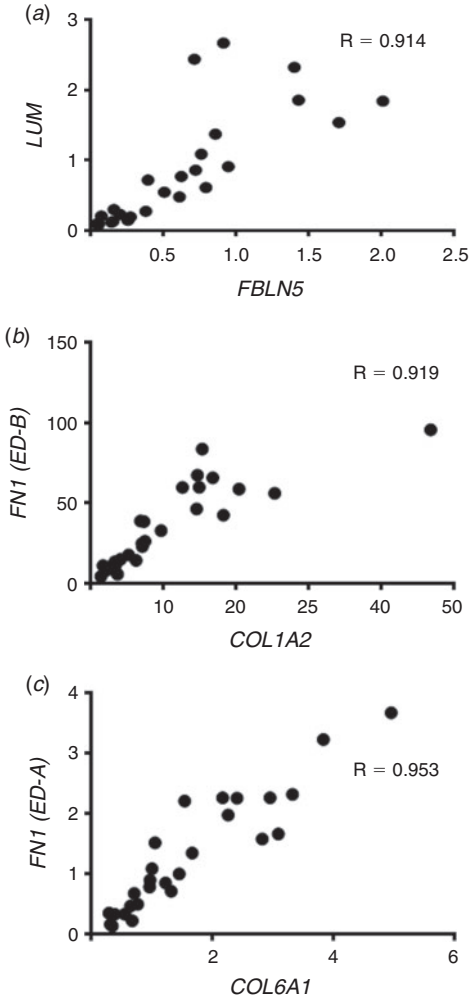

Fig. 5. Scatter plots showing related mRNA expression levels of (*a*) *LUM* versus *FBLN5*, (*b*) *FN1-EDB* versus *COL1A2* and (*c*) *FN1-EDA* versus *COL6A2* in whole bovine fetal ovaries. One ovary from each pair was used for mRNA analysis ($n = 27$ pairs). Data are presented as normalised gene expression to *GAPDH*. Spearman's correlation coefficient (R) test was used to analyse the data.

increase in stroma expansion across gestation but this rate of expansion slowed after Stage III. These rates of expansion are mirrored by the proliferation of stromal cells, but not the proportion of extracellular space, suggesting that stromal cell proliferation is largely responsible for stromal expansion during ovarian development.

Since stroma has been shown to expand significantly during ovarian development, genes that encode extracellular matrix proteins that might be involved in the expansion of the ovarian stroma were examined. Small leucine-rich proteoglycans (*SLRP*s) have a role in regulating collagen type I fibrillogenesis, which has been shown to be expressed during ovarian development in the rat (Paranko 1987) and cow (Hummitzsch *et al.* 2013). There are three classes of *SLRP*, Class I, Class II and Class III, which consist of extracellular matrix proteins, including asporin (*ASPN*) and biglycan (*BGN*), lumican (*LUM*) and

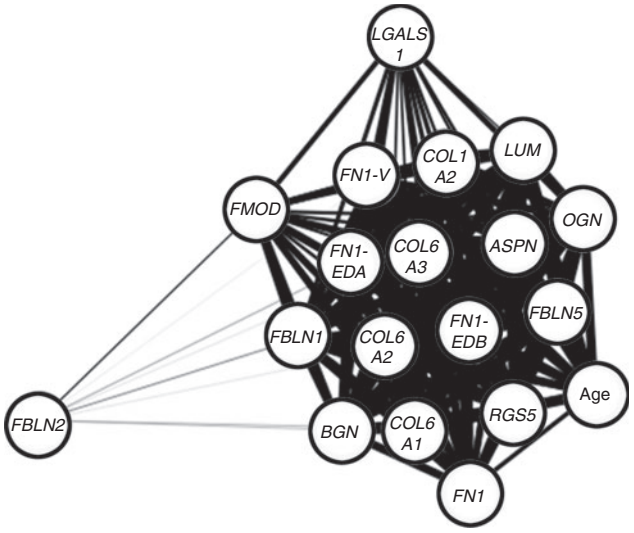

Fig. 6. An adjacent matrix network graph using correlation coefficients from Table 5. The closeness of the genes and the thickness of the interconnecting lines indicate stronger correlations between genes. Age is age of gestation.

fibromodulin (*FMOD*) and osteoglycin (*OGN*; Ameye and Young 2002). *ASPN* and *BGN* have been shown to be involved in collagen type I fibrillogenesis in human embryonic kidney cells and adult mouse ovary respectively (Oksjoki *et al.* 1999; Kalamajski *et al.* 2009). Another study showed that *LUM* and *FMOD* bind to collagen type I in an antagonistic manner during tendon development, which might be related to the formation of progressively thicker collagen fibrils (Kalamajski and Oldberg 2009). Additionally, *OGN* is involved in regulating collagen type I fibrillogenesis in mouse embryo fibroblasts (Ge *et al.* 2004). Since collagen type I also increases as the stroma expands during ovarian development, our findings indicate that *ASPN*, *LUM* and *OGN* might be involved in the deposition and assembly of extracellular matrix in stroma in bovine fetal ovary.

The establishment and the remodelling of the ovarian vascular system is required for development of the ovary (Robinson *et al.* 2009). Initially the penetration and expansion of the mesonephric stroma into the developing ovary brings with it capillaries contained therein (Hummitzsch *et al.* 2013; Smith *et al.* 2014). It has been shown that *RGS5* and *FBLN5*, which encode regulator of G-protein signalling 5 and fibulin 5 protein respectively, are involved in vascular remodelling (Berger *et al.* 2005; Spencer *et al.* 2005). RGS5 protein is a pericyte marker observed in the vasculature of mouse ovarian follicles (Berger *et al.* 2005), rat cerebral capillaries (Kirsch *et al.* 2001) and mouse embryonic pericytes (Bondjers *et al.* 2003). Pericytes have been observed in 23–24 week human fetal ovary as a part of a vascular network in the stroma (Niculescu *et al.* 2011). Additionally, a study using *FBLN5* knockout mice suggests the important role of *FBLN5* in neointima formation and vascular remodelling after an induced vascular injury (Spencer *et al.* 2005). Since the interaction between endothelial cells, pericytes and smooth muscle cells is critical for the development of the vasculature (Niculescu *et al.* 2011), the increased expression of *RGS5* and *FBLN5* suggests that these genes may play a role in expansion of the vasculature in the cortical stroma.

COL6A1, *COL6A2* and *COL6A3* encode the extracellular matrix component collagen type VI, which is predicted to help in anchoring tissues and cells to the connective tissue extracellular matrix (Cescon *et al.* 2015). In human adult ovary, collagen type VI is observed in the thecal layer, especially in the theca externa, and has a role in the interactions between the thecal cell and extracellular matrix during folliculogenesis (Iwahashi *et al.* 2000). A study using a yeast two-hybrid system showed an interaction between collagen type VI and collagen type IV (Kuo *et al.* 1997), which is localised in follicular basal lamina during ovarian development (Hummitzsch *et al.* 2013). Additionally, collagen type VI also interacts with other extracellular matrix components, such as collagen type I (Bonaldo *et al.* 1990) and fibronectin (Sabatelli *et al.* 2001). A study in the bovine fetal ovary showed that collagen type I and fibronectin were specifically expressed in the ovarian stroma (Hummitzsch *et al.* 2013), suggesting that collagen type VI might have an important role in anchoring vasculature in the stroma during the late stage of ovarian development.

FN1 encodes fibronectin, which modulates cell–cell and cell–matrix interactions (Goldberg *et al.* 2006). Fibronectin is composed of three structurally homologous types of repeated domains: Type I, II and III. Three different alternative splicing regions are located in Type III fibronectin: extra domain A (ED-A), B (ED-B) and the variable (V) region, encoded by *FN1-EDA*, *FN1-EDB* and *FN1-V*, respectively, (the variable region can have three to five alternative splicing events). The ED-A, ED-B and V regions are located between the 11th and 12th, between the 7th and 8th and between the 14th and 15th Type III repeats respectively (De Candia and Rodgers 1999). Collectively, these alternative splicing events potentially produce multiple different isoforms in humans, cows, mice and rats: ED-A+, ED-A–, ED-B+, ED-B–, V+ and V–. These have been shown to be expressed in bovine antral follicles of 0.5–9 mm diameter, in corpora lutea and in fetal bovine liver, lung and kidney but fetal ovaries were not examined in that study (De Candia and Rodgers 1999). The ED-A+ isoform has been identified in ovarian follicles and is predicted to be associated with the replication of granulosa cells (Colman-Lerner *et al.* 1999), whereas the ED-B+ and V+ isoforms have been shown to be involved in angiogenesis (Castellani *et al.* 1994; De Candia and Rodgers 1999). It is possible that the isoforms of FN1 might be involved in follicle formation and angiogenesis during ovarian development.

Many of the genes examined in the present study were highly positively correlated with gestational age and also with each other. This is not surprising as many of these genes were extracellular matrix genes associated with stroma, which also expanded during fetal development. Comparisons with earlier studies of bovine fetal ovaries (Hatzirodos *et al.* 2011) showed that fibrillin 3, another extracellular matrix gene that is familiarly linked to PCOS, is highly expressed only in the first trimester and declines in expression thereafter. This is interesting as fibrillin 3 is thus expressed in the fetal cortical stroma when it is proportionally expanding the most during fetal development. Why this particular gene should exhibit this

behaviour and not other stromal extracellular matrix genes is not known, but it does suggest that fibrillin 3 may have a unique role during ovarian cortical stroma expansion.

In summary we have shown quantitatively that the rate of expansion of cortical stroma is greatest early in development when the stroma penetrates the ovarian primordium from the mesonephros. The expansion of the cortical stroma occurs due to cell proliferation and not a change in cell size or a change in the amount of extracellular space. The mRNA expression levels of many extracellular matrix genes increased in the later stages of ovarian development and were highly correlated with each other, suggesting that they might be co-regulated. In conclusion, the behaviour of stroma changes during ovarian development and this might have consequences for its roles.

Conflicts of interest

The authors declare that there is no conflict of interest that could be perceived as prejudicing the impartiality of the research reported.

Acknowledgements

This research was funded by the Australia Awards Scholarship from the Australian Government, The University of Adelaide, the National Health and Medical Research Council (NHMRC) of Australia, the NHMRC Centre for Research Excellence in the Evaluation, Management and Health Care Needs of Polycystic Ovary Syndrome, the Society for Reproductive Biology and the Robinson Research Institute. We would like to acknowledge the Australian Research Council, Griffith University, S. Kidman and Co. and Ridley Agriproducts Pty Ltd for also funding this research. We would like to thank Thomas Food International, Murray Bridge, South Australia for providing the bovine tissues for this research.

References

Abbott, D. H., Padmanabhan, V., and Dumesic, D. A. (2006). Contributions of androgen and estrogen to fetal programming of ovarian dysfunction. *Reprod. Biol. Endocrinol.* **4**, 17. doi:10.1186/1477-7827-4-17

Adams, G. P., and Pierson, R. A. (1995). Bovine model for study of ovarian follicular dynamics in humans. *Theriogenology* **43**(1), 113–120. doi:10.1016/0093-691X(94)00015-M

Ameye, L., and Young, M. F. (2002). Mouse deficient in small leucine-rich proteoglycans novel *in vivo* models for osteoporosis, osteoarthritis, Ehlers–Danlos syndrome, muscular dystrophy, and corneal diseases. *Glycobiology* **12**(9), 107R–116R. doi:10.1093/GLYCOB/CWF065

Bandeira, F. T., Carvalho, A. A., Castro, S. V., Lima, L. F., Viana, D. A., Evangelista, J., Pereira, M., Campello, C. C., Figueiredo, J. R., and Rodrigues, A. (2015). Two methods of vitrification followed by *in vitro* culture of the ovine ovary: evaluation of the follicular development and ovarian extracellular matrix. *Reprod. Domest. Anim.* **50**(2), 177–185. doi:10.1111/RDA.12463

Bastian, N. A., Bayne, R. A., Hummitzsch, K., Hatzirodos, N., Bonner, W. M., Hartanti, M. D., Irving-Rodgers, H. F., Anderson, R. A., and Rodgers, R. J. (2016). Regulation of fibrillins and modulators of TGFβ in fetal bovine and human ovaries. *Reproduction* **152**, 127–137. doi:10.1530/REP-16-0172

Berger, M., Bergers, G., Arnold, B., Hammerling, G. J., and Ganss, R. (2005). Regulator of G-protein signaling-5 induction in pericytes coincides with active vessel remodeling during neovascularization. *Blood* **105**, 1094–1101. doi:10.1182/BLOOD-2004-06-2315

Berisha, B., Pfaffl, M. W., and Schams, D. (2002). Expression of estrogen and progesterone receptors in the bovine ovary during estrous cycle and pregnancy. *Endocrine* **17**, 207–214. doi:10.1385/ENDO:17:3:207

Berkholtz, C. B., Lai, B. E., Woodruff, T. K., and Shea, L. D. (2006). Distribution of extracellular matrix proteins type I collagen, type IV collagen, fibronectin, and laminin in mouse folliculogenesis. *Histochem. Cell Biol.* **126**(5), 583–592. doi:10.1007/S00418-006-0194-1

Bonaldo, P., Russo, V., Bucciotti, F., Doliana, R., and Colombatti, A. (1990). Structural and functional features of the alpha3 chain indicate a bridging role for chicken collagen VI in connective tissues. *Biochemistry* **29**(5), 1245–1254. doi:10.1021/BI00457A021

Bondjers, C., Kalén, M., Hellström, M., Scheidl, S. J., Abramsson, A., Renner, O., Lindahl, P., Cho, H., Kehrl, J., and Betsholtz, C. (2003). Transcription profiling of platelet-derived growth factor-B-deficient mouse embryos identifies RGS5 as a novel marker for pericytes and vascular smooth muscle cells. *Am. J. Pathol.* **162**(3), 721–729. doi:10.1016/S0002-9440(10)63868-0

Castellani, P., Viale, G., Dorcaratto, A., Nicolo, G., Kaczmarek, J., Querze, G., and Zardi, L. (1994). The fibronectin isoform containing the ED-B oncofetal domain: a marker of angiogenesis. *Int. J. Cancer* **59**, 612–618. doi:10.1002/IJC.2910590507

Cescon, M., Gattazzo, F., Chen, P., and Bonaldo, P. (2015). Collagen VI at a glance. *J. Cell Sci.* **128**(19), 3525–3531. doi:10.1242/JCS.169748

Colman-Lerner, A., Fischman, M. L., Lanuza, G. M., Bissel, D. M., Kornblihtt, A. R., and Baranao, J. L. (1999). Evidence for a role of the alternatively spliced ED-I sequence of fibronectin during ovarian follicular development. *Endocrinology* **140**(6), 2541–2548. doi:10.1210/ENDO.140.6.6708

Copping, K. J., Hoare, A., Callaghan, M., McMillen, I. C., Rodgers, R. J., and Perry, V. E. A. (2014). Fetal programming in 2-year-old calving heifers: peri-conception and first trimester protein restriction alters fetal growth in a gender-specific manner. *Anim. Prod. Sci.* **54**, 1333–1337.

De Candia, L. M., and Rodgers, R. J. (1999). Characterization of the expression of the alternative splicing of the ED-A, ED-B and V regions of fibronectin mRNA in bovine ovarian follicles and corpora lutea. *Reprod. Fertil. Dev.* **11**, 367–377. doi:10.1071/RD99087

Epskamp, S., Cramer, A. O. J., Waldorp, L. J., Schmittmann, V. D., and Borsboom, D. (2012). qgraph: network visualizations of relationships in psychometric data. *J. Stat. Softw.* **48**(4), 1–18. doi:10.18637/JSS.V048.I04

Figueiredo, J. R., Hulshof, S. C. J., Thiry, M., Van den Hurk, R., Bevers, M. M., Nusgens, B., and Beckers, J. F. (1995). Extracellular matrix proteins and basement membrane: their identification in bovine ovaries and significance for the attachment of cultured preantral follicles. *Theriogenology* **43**, 845–858. doi:10.1016/0093-691X(95)00036-8

Fulghesu, A. M., Clampelli, M., Belosi, C., Apa, R., Pavone, V., and Lanzone, A. (2001). A new ultrasound criterion for the diagnosis of polycystic ovary syndrome: the ovarian stroma/total area ratio. *Fertil. Steril.* **76**(2), 326–331. doi:10.1016/S0015-0282(01)01919-7

Ge, G., Seo, N. S., Liang, X., Hopkins, D. R., Hook, M., and Greenspan, D. S. (2004). Bone morphogenetic protein-1/tolloid-related metalloproteinases process osteoglycin and enhance its ability to regulate collagen fibrillogenesis. *J. Biol. Chem.* **279**(40), 41626–41633. doi:10.1074/JBC.M406630200

Goldberg, M., Septier, D., Oldberg, A., Young, M. F., and Ameye, L. G. (2006). Fibromodulin-deficient mice display impaired collagen fibrillogenesis in predentin as well as altered dentin mineralization and enamel formation. *J. Histochem. Cytochem.* **54**(5), 525–537. doi:10.1369/JHC.5A6650.2005

Hatzirodos, N., Bayne, R. A., Irving-Rodgers, H. F., Hummitzsch, K., Sabatier, L., Lee, S., Bonner, W., Gibson, M. A., Rainey, W. E., Carr, B. R., Mason, H. D., Reinhardt, D. P., Anderson, R. A., and Rodgers, R. J. (2011). Linkage of regulators of TGF-beta activity in the fetal ovary to polycystic ovary syndrome. *FASEB J.* **25**(7), 2256–2265. doi:10.1096/FJ.11-181099

Heeren, A. M., van Iperen, L., Klootwijk, D. B., de Melo Bernardo, A., Roost, M. S., Gomes Fernandes, M. M., Louwe, L. A., Hilders, C. G., Helmerhorst, F. M., van der Westerlaken, L. A., and Chuva de Sousa Lopes, S. M. (2015). Development of the follicular basement membrane during human gametogenesis and early folliculogenesis. *BMC Dev. Biol.* **15**, 4. doi:10.1186/S12861-015-0054-0

Huet, C., Pisselet, C., Mandon-Pépin, B., Monget, P., and Monniaux, D. (2001). Extracellular matrix regulates ovine granulosa cell survival, proliferation and steroidogenesis: relationships between cell shape and function. *J. Endocrinol.* **169**, 347–360. doi:10.1677/JOE.0.1690347

Hughesdon, P. E. (1982). Morphology and morphogenesis of the Stein–Leventhal ovary and of so-called "hyperthecosis". *Obstet. Gynecol. Surv.* **37**(2), 59–77. doi:10.1097/00006254-198202000-00001

Hummitzsch, K., Irving-Rodgers, H. F., Hatzirodos, N., Bonner, W., Sabatier, L., Reinhardt, D. P., Sado, Y., Ninomiya, Y., Wilhelm, D., and Rodgers, R. J. (2013). A new model of development of the mammalian ovary and follicles. *PLoS One* **8**(2), e55578. doi:10.1371/JOURNAL.PONE.0055578

Hummitzsch, K., Anderson, R. A., Wilhelm, D., Wu, J., Telfer, E. E., Russell, D. L., Robertson, S. A., and Rodgers, R. J. (2015). Stem cells, progenitor cells, and lineage decisions in the ovary. *Endocr. Rev.* **36**(1), 65–91. doi:10.1210/ER.2014-1079

Irving-Rodgers, H. F., and Rodgers, R. J. (2007). Extracellular matrix in ovarian follicular and luteal development. In 'Novel Concepts in Ovarian Endocrinology'. (Ed. A. Gonzalez-Bulnes.) pp. 83–112. (Transworld Research Network: Kerala, India.)

Irving-Rodgers, H. F., Bathgate, R. A. D., Ivell, R., Domagalski, R., and Rodgers, R. J. (2002). Dynamic changes in the expression of relaxin-like factor (Insl3), cholesterol side-chain cleavage cytochrome p450, and 3beta-hydroxysteroid dehydrogenase in bovine ovarian follicles during growth and atresia. *Biol. Reprod.* **66**, 934–943. doi:10.1095/BIOLREPROD66.4.934

Iwahashi, M., Muragaki, Y., Ooshima, A., and Nakano, R. (2000). Type VI collagen expression during growth of human ovarian follicles. *Fertil. Steril.* **74**(2), 343–347. doi:10.1016/S0015-0282(00)00618-X

Kagawa, N., Silber, S., and Kuwayama, M. (2009). Successful vitrification of bovine and human ovarian tussue. *Reprod. Biomed. Online* **18**, 568–577. doi:10.1016/S1472-6483(10)60136-8

Kalamajski, S., and Oldberg, A. (2009). Homologous sequence in lumican and fibromodulin leucine-rich repeat 5–7 competes for collagen binding. *J. Biol. Chem.* **284**(1), 534–539. doi:10.1074/JBC.M805721200

Kalamajski, S., Aspberg, A., Lindblom, K., Heinegard, D., and Oldberg, A. (2009). Asporin competes with decorin for collagen binding, binds calcium and promotes osteoblast collagen mineralization. *Biochem. J.* **423**(1), 53–59. doi:10.1042/BJ20090542

Kirsch, T., Wellner, M., Luft, F. C., Haller, H., and Lippoldt, A. (2001). Altered gene expression in cerebral capillaries of stroke-prone spontaneously hypertensive rats. *Brain Res.* **910**, 106–115. doi:10.1016/S0006-8993(01)02670-1

Kobayashi, H., Sun, W. G., and Terao, T. (1999). Immunolocalization of hyaluronic acid and inter-alpha-trypsin inhibitor in mice. *Cell Tissue Res.* **296**, 587–597. doi:10.1007/S004410051320

Kuo, H.-J., Maslen, C. L., Keene, D. R., and Glanville, R. W. (1997). Type VI collagen anchors endothelial basement membranes by interacting with type IV collagen. *J. Biol. Chem.* **272**(42), 26522–26529. doi:10.1074/JBC.272.42.26522

Li, Z., and Huang, H. (2008). Epigenetic abnormality: a possible mechanism underlying the fetal origin of polycystic ovary syndrome. *Med. Hypotheses* **70**(3), 638–642. doi:10.1016/J.MEHY.2006.09.076

Lind, A. K., Weijdegard, B., Dahm-Kahler, P., Molne, J., Sundfeldt, K., and Brannstrom, M. (2006). Collagens in the human ovary and their changes in the perifollicular stroma during ovulation. *Acta Obstet. Gynecol. Scand.* **85**(12), 1476–1484. doi:10.1080/00016340601033741

Loverro, G., De Pergola, G., Di Naro, E., Tartagni, M., Lavopa, C., and Caringella, A. M. (2010). Predictive value of ovarian stroma measurement for cardiovascular risk in polycyctic ovary syndrome: a case control study. *J. Ovarian Res.* **3**, 25. doi:10.1186/1757-2215-3-25

Matti, N., Irving-Rodgers, H. F., Hatzirodos, N., Sullivan, T. R., and Rodgers, R. J. (2010). Differential expression of focimatrix and steroidogenic enzymes before size deviation during waves of follicular development in bovine ovarian follicles. *Mol. Cell. Endocrinol.* **321**(2), 207–214. doi:10.1016/J.MCE.2010.02.019

McArthur, M. E., Irving-Rodgers, H. F., Byers, S., and Rodgers, R. J. (2000). Identification and immunolocalization of decorin, versican, perlecan, nidogen, and chondroitin sulfate proteoglycans in bovine small-antral ovarian follicles. *Biol. Reprod.* **63**, 913–924. doi:10.1095/BIOLREPROD63.3.913

Niculescu, M., Novac, L., Mateescu, G. O., Mihail, S. R., Neamtu, S., and Papachristu, A. (2011). Original study the vasculogenesis of the fetal ovary – morphological and immunohistochemical study. *Analele Universitatii "Dunarea De Jos" Galati Medicina* **17**(1), 5–9.

Oksjoki, S., Sallinen, S., Vuorio, E., and Anttila, L. (1999). Cyclic expression of mRNA transcripts for connective tissue components in the mouse ovary. *Mol. Hum. Reprod.* **5**(9), 803–808. doi:10.1093/MOLEHR/5.9.803

Paranko, J. (1987). Expression of type I and III collagen during morphogenesis of fetal rat testis and ovary. *Anat. Rec.* **219**, 91–101. doi:10.1002/AR.1092190115

Prodoehl, M. J., Irving-Rodgers, H. F., Bonner, W. M., Sullivan, T. M., Micke, G. C., Gibson, M. A., Perry, V. E., and Rodgers, R. J. (2009). Fibrillins and latent TGFbeta binding proteins in bovine ovaries of offspring following high or low protein diets during pregnancy of dams. *Mol. Cell. Endocrinol.* **307**(1–2), 133–141. doi:10.1016/J.MCE.2009.03.002

Robinson, R. S., Woad, K. J., Hammond, A. J., Laird, M., Hunter, M. G., and Mann, G. E. (2009). Angiogenesis and vascular function in the ovary. *Reproduction* **138**(6), 869–881. doi:10.1530/REP-09-0283

Roy, S. K., and Kole, A. R. (1998). Ovarian transforming growth factor-b (TGF-b) receptors: *in vitro* effects of follicle stimulating hormone, epidermal growth factor and TGF-b on receptor expression in human preantral follicles. *Mol. Hum. Reprod.* **4**(3), 207–214. doi:10.1093/MOLEHR/4.3.207

Rozen, S., and Skaletsky, H. J. (2000). Primer3 on the WWW for general users and for biologist programmers. In 'Bioinformatics methods and protocols: methods in molecular biology'. (Eds S. Krawetz and S. Misener.) pp. 365–386. (Humana Press: Totowa, NJ, USA.)

Russe, I. (1983). Oogenesis in cattle and sheep. *Bibl. Anat* **24**, 77–92.

Sabatelli, P., Bonaldob, P., Lattanzia, G., Braghettab, P., Bergaminb, N., Capannic, C., Mattiolid, E., Columbarod, M., Ognibenec, A., Pepee, G., Bertinif, E., Merlinid, L., Maraldia, N. M., and Squarzonia, S. (2001). Collagen VI deficiency affects the organization of fibronectin in the extracellular matrix of cultured fibroblasts. *Matrix Biol.* **20**(7), 475–486. doi:10.1016/S0945-053X(01)00160-3

Santos, S. S., Ferreira, M. A., Pinto, J. A., Sampaio, R. V., Carvalho, A. C., Silva, T. V., Costa, N. N., Cordeiro, M. S., Miranda, M. S., Ribeiro, H. F., and Ohashi, O. M. (2013). Characterization of folliculogenesis and the occurrence of apoptosis in the development of the bovine fetal ovary. *Theriogenology* **79**(2), 344–350. doi:10.1016/J.THERIOGENOLOGY.2012.09.026

Sarraj, M. A., and Drummond, A. E. (2012). Mammalian foetal ovarian development: consequences for health and disease. *Reproduction* **143**(2), 151–163. doi:10.1530/REP-11-0247

Schindelin, J., Arganda-Carreras, I., Frise, E., Kaynig, V., Longair, M., Pietzsch, T., Preibisch, S., Rueden, C., Saalfeld, S., Schmid, B., Tinevez, J.-Y., White, D. J., Hartenstein, V., Eliceiri, K., Tomancak, P., and

Cardona, A. (2012). Fiji: an open-source platform for biological-image analysis. *Nat. Methods* **9**(7), 676–682. doi:10.1038/NMETH.2019

Sforza, C., Ferrario, V. F., De Pol, A., Marzona, L., Forni, M., and Forabosco, A. (1993). Morphometric study of the human ovary during compartmentalization. *Anat. Rec.* **236**, 626–634. doi:10.1002/AR.1092360406

Smith, P., Wilhelm, D., and Rodgers, R. J. (2014). Development of mammalian ovary. *J. Endocrinol.* **221**(3), R145–R161. doi:10.1530/JOE-14-0062

Spencer, J. A., Hacker, S. L., Davis, E. C., Mecham, R. P., Knutsen, R. H., Li, D. Y., Gerard, R. D., Richardson, J. A., Olson, E. N., and Yanagisawa, H. (2005). Altered vascular remodeling in fibulin-5-deficient mice reveals a role of fibulin-5 in smooth muscle cell proliferation and migration. *Proc. Natl. Acad. Sci. USA* **102**(8), 2946–2951. doi:10.1073/PNAS.0500058102

Wandji, S. A., Sršeň, V., Voss, A. K., Eppig, J. J., and Fortune, J. E. (1996). Initiation *in vitro* of growth of bovine primordial follicles 1. *Biol. Reprod.* **55**(5), 942–948. doi:10.1095/BIOLREPROD55.5.942

Weng, Q., Wang, H., Medan, M. S., Jin, W., Xia, G., Watanabe, G., and Taya, K. (2006). Expression of inhibin-activin subunits in the ovaries of fetal and neonatal mice. *J. Reprod. Dev.* **52**(5), 607–616. doi:10.1262/JRD.18026